J Therm Anal Calorim (2010) 102:269–275
DOI 10.1007/s10973-009-0446-0

Characterization of the indinavir raw materials stability in some pharmaceutical processes

Ticiano Gomes do Nascimento · Irinaldo D. Basílio Júnior · Rui O. Macêdo · Elisana A. Moura · Camila B. Dornelas · Vanderson B. Bernardo · Vânia N. Rocha · Csaba Nóvak

Received: 13 July 2009 / Accepted: 25 August 2009 / Published online: 11 September 2009

Abstract This article characterizes the stability of indinavir sulfate using different analytical techniques of quality control to evaluate important steps in the manufacturing process of indinavir, specifically involving storage and compression. Indinavir A, B, and C were obtained from different suppliers and submitted to DSC, Karl Fisher, NIR, XRPD analyses and dissolution assay. DSC curves of indinavir presented endothermic peaks of fusion at 149–150 °C for indinavir A and B (form I) and 139–143 °C for indinavir C (form II). When indinavir A and B were submitted to high Relative Humidity (RH) pseudo-polymorphic form II was formed. Indinavir C converted into an amorphous substance when submitted to compression. Near infrared and Karl Fisher assays detected high values of water for indinavir C in relation to indinavir A and B. X-ray powder diffraction of indinavir B and C showed displacement of 0.05–0.10 θ in the peaks and higher angle of diffraction in relation to indinavir A. Amorphous indinavir C demonstrated a higher intrinsic dissolution rate than indinavir A and B. Indinavir form I should be monitored during the pharmaceutical process to avoid its conversion to indinavir form II or an amorphous substance which can alter the dissolution rate.

Keywords Indinavir sulfate · Stability of hydrates · DSC · Intrinsic dissolution · Raw materials

T. G. do Nascimento (✉) · I. D. Basílio Júnior · C. B. Dornelas · V. B. Bernardo
Laboratório de Controle de Qualidade de Fármacos e Medicamentos, Grupo de Pesquisa em Tecnologia e Controle de Qualidade de Medicamentos, Escola de Enfermagem e Farmácia, Universidade Federal de Alagoas—UFAL, Campus A. C. Simões, Br 104 Norte, Km 97, Maceió, Estado de Alagoas CEP 57072-970, Brazil
e-mail: ticianogn@yahoo.com.br

R. O. Macêdo · E. A. Moura
Laboratórios Unificados de Desenvolvimento e Ensaios de Medicamentos, Departamento de Ciências Farmacêuticas, Universidade Federal da Paraíba—UFPB, Campus I, João Pessoa, Estado da Paraíba CEP 58059-900, Brazil

V. N. Rocha
Laboratório Industrial Farmacêutico do Estado de Alagoas—LIFAL, Av. Salvador Lira s/n, Distrito Industrial Governador Luis Cavalcante, Tabuleiro dos Martins, Maceió, Estado de Alagoas CEP 57082-000, Brazil

C. Nóvak
Hungarian Academy of Sciences, Budapest University of Technology and Economics, Research Group of Technical Analytical Chemistry, Szt. Gellért tér 4, 1111 Budapest, Hungary

Introduction

Indinavir sulfate is chemically known as [1(1*S*,2*R*),5(*S*)]-2,3,5-trideoxy-*N*-(2,3-dihydro-2-hydroxy-1*H*-inden-1-yl)-5-[2-[[(1,1-dimethylethyl)amino] carbonyl]-4-(3-pyridinylmethyl)-1-piperazinyl]-2-phenylmethyl)-D-*erythro*-pentonamide sulfate (1:1) salt. Indinavir sulfate is a white crystalline powder and can also be an amorphous powder. This drug is soluble in water, ethanol, but is poorly soluble in acetonitrile and dichloromethane [1].

The efficacy of antiretroviral therapy is often monitored to evaluate the patient adhesion to treatment due to the possibility of toxicological risks and adverse reaction [2]. The quality of the indinavir raw materials and their related compounds must be monitored by the pharmaceutical industry to minimize the adverse effects and increase the quality assurance of the product and its therapeutic efficacy [3]. The department of quality assurance in the pharmaceutical industry has a compromise in maintaining a

qualification program of raw material suppliers, a validation program of the manufacturing process and the monitoring program of drug stability. These programs are critical to the pharmaceutical manufacturing process and involve a high productive cost, qualification of personnel, as well as the adequate analytic techniques for specificity of drugs aimed at attending the Good Manufacture Practices of the pharmaceutical industry.

The term pseudo-polymorphism relates to the phenomenon of incorporation of solvent molecules into crystal lattice or crystal interstitial voids. Hydrates represent different chemical entities as defined by the stoichiometry of water with respect to the active compound. Depending upon the nature of the hydrate, the water content may change over time with the environmental humidity, temperature, or other processing conditions [4]. The behavior of pharmaceutical hydrates has become the object of increasing attention over the past decade, primarily due (directly or indirectly) to the potential impact of hydrates on the development process and the dosage form performance [5]. Specifically, pseudo-polymorphic forms can develop in pharmaceuticals after long storage periods [6], grinding, milling and through the tabletting process which can promote modifications on the melting point, solubility, dissolution rate, and bioavailability of drugs [7].

Quality control of the raw materials is necessary to ensure the batch-to-batch quality of pharmaceutical products and DSC and TG have been used for this purpose. Thermal analysis has been used in the development of solid pharmaceutical forms [8, 9], in the evaluating of stability of the raw materials [10] and in the investigation of polymorphism and pseudo-polymorphism in pharmaceuticals [3, 11]. Besides thermal analysis, other analytical techniques are also used in characterization of crystalline pharmaceutical polymorphs and hydrates, which exhibited physical differences in medium infrared and near infrared, X-ray powder diffraction patterns, NMR, dissolution rates, and hygroscopicity [5, 12–15].

Intrinsic Dissolution Rate (IDR) is used to characterize solid pharmaceutical drugs [16, 17]. Many studies proved the IDR to characterize polymorphic, pseudo-polymorphic, and amorphous drug substances [6, 14, 15]. Therefore, IDR can be applied as a main tool in preformulation studies and in the establishment of the solubility classification method as an auxiliary to the biopharmaceutical classification system [18].

Indinavir demonstrated industrial problems during process ability due to its instability to heat, relative humidity, storage, and the mechanical process. Thus, the present study shows the importance of the characterization of indinavir raw materials using different analytical techniques to solve industrial problems and to assure the solid state stability of indinavir as indicative of quality guarantee during some steps of productive pharmaceutical chain.

Experimental

Indinavir samples

The samples of indinavir sulfate (IS) drug substance were donated by LIFAL from three different suppliers and submitted to thermal analysis, Karl Fisher, near infrared, X-ray powder diffraction and dissolution studies without previous treatment.

The samples of indinavir A (Lot. IS5005-08-003), indinavir B (Lot. DH 78-4-060701) and Indinavir C (Lot. IIS-C0650044) were obtained by suppliers A (Zhejiang®; China), B (Shangai Desano®; China) and C (Aurobindo Pharma®; India), respectively.

Differential scanning calorimetry (DSC)

The DSC curves of IS were performed in a Shimadzu calorimeter (Tokyo, Japan), model DSC-60, at a heating rates of 10 °C min^{-1}, under nitrogen atmosphere, and a temperature range of 25–500 °C. The samples (2.00 mg ± 10%) were packed in an aluminum crucible. The crucible was sealed hermetically. The DSC temperature and heat flow were calibrated by the melting point and enthalpy of fusion from indium and zinc standards.

X-ray powder diffraction (XRPD)

X-ray powder diffraction was used to confirm the pseudo-polymorphic forms of indinavir sulfate in the raw materials. The diffraction patterns were recorded by using a θ–θ X-ray powder diffractometer (Rigaku, model Miniflex, Tokyo, Japan), equipped with a Göbel mirror bent multilayer optic. Measurements were performed in a symmetrical reflection mode with Cu $K\alpha$ radiation at 40 kV and 30 mA. The powders of indinavir were scanned in an angular range of 2° (2θ) to 30° (2θ) with the step size of 0.05° (2θ).

Near infrared (NIR)

The NIR spectra were recorded using a NIR spectrometer from Varian (Palo Alto, CA, USA), model Scimitar 2000 series, using a reflectance diffuse cell and programed in Varian Software. The apparatus was adjusted with interferometer of 8.00, using a scan of blank. The equipment was programed to collect the spectra with the number of 64 scans over a wavelength range of 10,000–4,000 cm^{-1}. The spectra were acquired in Kubelka–Munk mode.

Karl Fisher

The water content of indinavir was determined using a Karl Fisher titrator from Mettler-Toledo (Columbus, OH, USA),

model DL38, and also using a Hydra-point solution (5.00 mg water/mL) and methanol for analysis, both from J.T. Baker (Phillipsburg, New Jersey, USA). The calibration was performed with freshly millipore water using a mass of 15.00 mg ± 1.30. After this calibration, indinavir A (107.20 mg ± 0.80), B (106.00 mg ± 2.60) and C (105.00 mg ± 2.50) were submitted to a Karl Fisher analysis in triplicate. The water content was determinate for the term of 12 and 36 h of exposition to 65% of RH.

Intrinsic dissolution and dissolution profile

Intrinsic dissolution rate was performed on all raw materials. The indinavir sulfate raw materials (250.0 mg) were submitted to a compression force of 20 kN under a hydraulic press for 1 min to produce pellets and assayed with a rotating disk apparatus in a die of 8 mm diameter. Intrinsic dissolution studies were performed in Nova Etica apparatus (São Paulo, Brazil) model 299, with 900 mL of dissolution media (HCl 0.1 M) at 37 ± 0.5 °C and 100 rpm. The times of collection were 3, 10, 20, 30, and 45 min. A volume of 10 mL of the medium was periodically withdrawn (with reposition) and the indinavir concentration was determined by UV spectroscopy at 260 nm. The intrinsic dissolution were designed to obtain a concentration of 0.04444 mg/mL, standard solutions of the drug were prepared to obtain a standard curve of absorption versus concentration. The sink condition was maintained and the intrinsic dissolution assay was evaluated in triplicate.

Indinavir A and C were also assayed in a dissolution profile similar to the indinavir capsule product. Indinavir sulfate raw materials were weighed precisely (500.0 mg), transferred to capsules (Capsugel, São Paulo, Brazil) and submitted to a 1,000 handmade compacting. The dissolution profiles were performed in the same equipment and same condition to intrinsic dissolution assay as described in Brazilian pharmacopeia IV [1].

Results and discussion

DSC curves

DSC curves of indinavir sulfate of the different suppliers presented three transitions in the temperatures ranges of 95–100, 142–149, and 200–320 °C. The first endothermic peak corresponded to the desolvation of water in the indinavir sulfate. The second endothermic peak showed the indinavir melt and the third endothermic peak was the decomposition of the indinavir (Fig. 1a). Indinavir C presented a peak of fusion at 143.6 °C, different from indinavir A at 149.1 °C, which is in agreement with the literature (150–153 °C) [19].

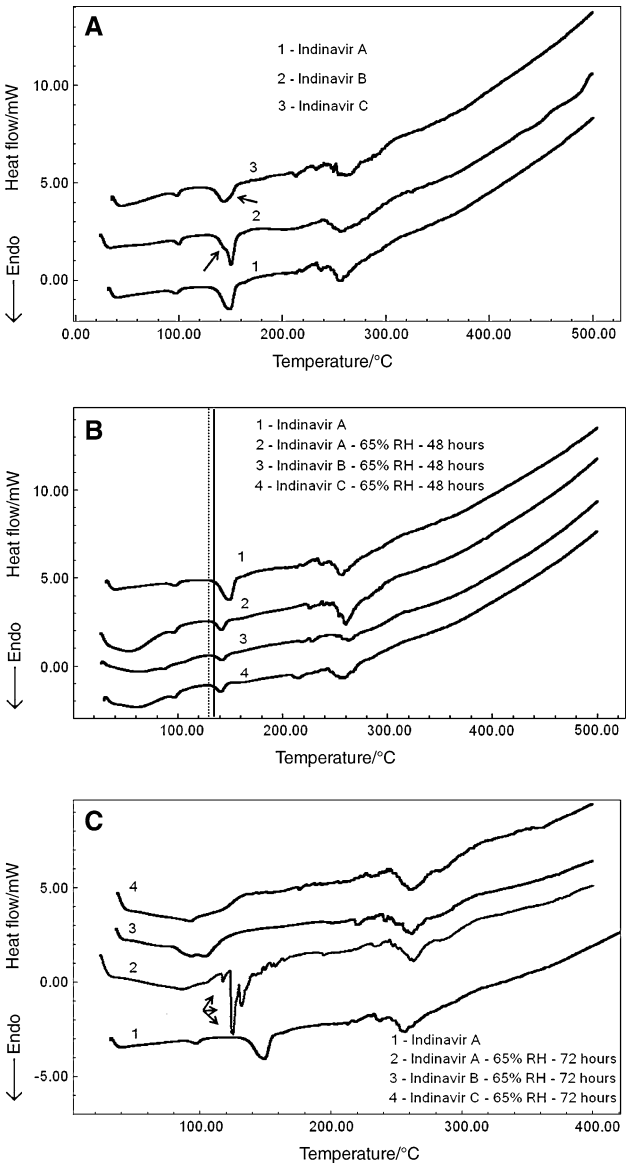

Fig. 1 DSC curves of indinavir recorded at 10 °C min^{-1} without previous treatment (**a**) and after exposure to 65% of relative humidity for 48 h (**b**) and for 72 h (**c**). *Solid line* indicates the Tonset of fusion peak for indinavir A and *dotted line* indicates the displacement Tonset of the fusion peak for indinavir after humidity exposure. The *arrows* show three transition peaks, which suggest degradation product in the indinavir A after long period of exposure to humidity

We observed that indinavir B melted at 150.5 °C similarly to indinavir A, but we detected a shoulder at 142.8 °C (Fig. 1a, curve 2). Indinavir C presented the same phenomenon similar to indinavir B with the peak of fusion at 143.6 °C and a shoulder at 151.2 °C when determined by tangent analyses from the Tasys Software (Shimadzu, Tokyo, Japan) (Fig. 1a, curve 3). These two ranges in the melting point of indinavir sulfate were previously demonstrated by Da Silva et al. [3]. Evaluating the calorimetric

data, it was possible to establish indinavir A as purity substance in our DSC analysis.

DSC data did not detect the presence of any indinavir degradation products in the samples without previous treatment. Cis-amino indanol has presented a melting point in the range of 118–121 °C according to literature [20]. Indinavir lactone was also investigated by DSC [21] with a melting point with decomposition detected in the range of 160–210 °C and mass loss in TG/DRTG curves, which can be related to indinavir lactone and other polymorphic forms of indinavir when submitted to thermal stress prior to DSC/TG analysis.

The stability of indinavir sulfate was characterized when submitted to drastic conditions in thermal stress [21] and forced degradation [22] in solution, photochemical stability, and thermal degradation. But in our experiments, indinavir sulfate was evaluated at normal and controlled storage conditions of relative humidity at room temperature for a long period. Thus, we observed the influence of relative humidity during a long period of storage on the physical–chemical stability of indinavir as indicative of quality for these raw materials.

Calorimetric data showed that there was a chemical equilibrium of the pseudo-polymorphic form I (peak of fusion at 147–150 °C) and pseudo-polymorphic form II (peak of fusion at 141–143 °C), but this chemical equilibrium is displacement for pseudo-polymorphic II during long term of storage. Other experiments were necessary to prove the conversion of the pseudo-polymorphic form I to pseudo-polymorphic form II.

The calorimetric data suggested an alteration in the peak of fusion during a long period of storage (1) or non-standardization in technology of the synthesis or purification process (2). Based on the first hypothesis (1) there were experimental evidences that indinavir changed the peak of fusion during the long period of storage.

We performed two additional experiments to prove our (1) first hypothesis. Indinavir raw materials were exposed to 65% of relative humidity at room temperature for 48 h (Fig. 1b) and for 72 h (Fig. 1c). Then, indinavir A, B, and C were submitted to DSC analysis. We detected a change in the peak of fusion for indinavir A (141.6 °C) and B (142.1 °C), which converted into pseudo-polymorphic II similar to indinavir C (140.8 °C). There were no reconversions in the pseudo-polymorphic I form of indinavir after dehydration in a temperature of 115 °C for 2 h. After 72 h, indinavir raw materials were transformed into a bright white solid. DSC did not present a peak of fusion for indinavir B and C demonstrating the presence of amorphous powders. But indinavir A revealed three peaks of transitions phase at 117.7, 124.6, and 130.7 °C (Fig. 1c) which suggests the presence of cis-amino indanol as degradation product of the indinavir. This fact revealed a large instability of indinavir when exposed to a high relative humidity.

Indinavir raw materials also were submitted to compression in a hydraulic press under a 20 kN force for 1 min. Then, indinavir raw materials were grounded, homogenized (with the use of a mortar and pistils), and submitted to the DSC analysis. The DSC curves also showed a displacement in the fusion peak of indinavir A (139.3 °C), indinavir B (139.0 °C), but indinavir C did not present a peak of fusion, proving that probably the high compression in the hydraulic press can convert the indinavir C into a amorphous substance. These accelerated experiments were in accordance with our first hypothesis: "Indinavir sulfate when submitted to a long period of storage or when exposed to humidity or when submitted to high compression force changes the range of the peak of fusion and consequently, there is a conversion of the pseudo-polymorphic form I into a pseudo-polymorphic form II" *or amorphous substance*. The experiment with high compression demonstrated that better attention should be taken during the mechanical compaction process to increase the powder density before filling capsule operation. This experiment also proves the difficulty on the manipulating of this active substance as a compressed tablet pharmaceutical form and preserving the physical–chemical proprieties.

X-ray powder diffraction

The X-ray powder diffraction showed eight main diffraction angles for all indinavir. In spite of a superposition of peaks of the diffraction angles, the XRPD data also showed circumstantial differences for indinavir sulfate. The samples B and C presented displacement of 0.05–0.10 θ in the peaks to a higher diffraction angle in relation to indinavir A, but indinavir C presented larger displacements than indinavir B (Table 1). These data confirmed that indinavir sulfate exists in two pseudo-polymorphic forms and not as two polymorphic forms. The presence of humidity in a crystal lattice can promote short alterations in the diffraction angles as described by Brittain [13] in the pharmaceutical hydrates. Indinavir showed differences in the diffraction angles with the increasing of the hydration grade.

Near infrared

The NIR spectra of the three indinavir showed a similarity. Displacement on the stretching was observed on the harmonic band at 5,164 cm^{-1} (indinavir A) and the increase in the intensity of response (area) demonstrated with indinavir B and C in relation to indinavir A. This fact can be attributed to higher interactions of hydrogen binding

Table 1 Analytical data of indinavir sulfate obtained by NIR and XRPD

Raw materials	NIR		XRPD	
	Frequency/ cm^{-1}	Area	Angle of diffraction (θ)	Intensity (CPS)
Indinavir A	6,541	5.95	5.90	4,311
	5,947	21.76	6.15	5,834
	5,164	**53.10**	8.05	2,100
	4,869	6.06	12.35	2,276
	4,659	3.80	16.15	3,791
	4,338	10.12	18.60	3,115
	4,210	4.95	19.40	2,579
	4,053	19.86	21.60	2,590
Indinavir B	6,546	9.11	5.95	3,957
	5,946	29.24	6.25	6,883
	5,158	**62.47**	8.10	2,227
	4,868	11.63	12.40	2,566
	4,659	4.57	16.15	4,178
	4,337	16.83	18.65	3,691
	4,207	8.84	19.45	2,846
	4,054	36.43	21.70	2,842
Indinavir C	6,542	6.16	6.00	2,981
	5,942	24.93	6.25	4,090
	5,172	**84.65**	8.10	1,396
	4,870	8.10	12.40	1,594
	4,659	4.62	16.20	2,742
	4,338	15.48	18.70	2,894
	4,210	6.93	19.50	2,512
	4,054	30.45	21.70	2,648

The bold values indicate the wavelength and correspondent area which identify the water amount in near infrared

between the hydroxyl group (OH) of hydration water and the indinavir molecule. Czarnik-Matusewicz and Pilorz [23] characterized water stretching as weaker and stronger in near infrared at 7,000 and 5,173 cm^{-1}, respectively. Indinavir C presented higher values of intensity of area in relation to other raw materials (Table 1). Analyses of the NIR spectrum were essential to prove the higher amount of water in indinavir C than indinavir A and B.

Karl Fisher titration

The amount of hydrate water was determined using Karl Fisher assay. Indinavir A, B, and C were totally soluble in methanol and presented values in the percentage of water (1.10% ± 0.06), (1.28% ± 0.14) and (1.85% ± 0.01), respectively. On the basis of this information, we observed differences in hydrate water of the indinavir. The indinavir:water ratios were (1:0.44), (1:0.51), (1:0.75) for indinavir A, B, and C, respectively. Thus, we can classify these raw materials as hemihydrates (indinavir A and B) with the peak of fusion at 149–150 °C and hydrate (indinavir C) with the peak of fusion at 139–143 °C.

Additional Karl Fisher assay was performed for indinavir when submitted to a high relative humidity of 65%. Indinavir A (8.53% ± 0.10; 9.06% ± 0.20), B (7.03% ± 0.07; 7.19% ± 0.17) and C (7.26% ± 0.04; 7.33% ± 0.22) presented a mass gain which represented a molar proportion between indinavir:water of (1:3.7; 1:4.0) for indinavir A, (1:3.0; 1:3.1) for indinavir B and (1:3.1; 1:3.1) for indinavir C, during the term of 12 and 36 h, respectively. The Karl Fisher analysis was in accordance with the DSC data due to the fact that after exposure of indinavir to a 65% of RH for 48 h, it was converted into hydrates forms.

Dissolution and intrinsic dissolution

No differences were found in the dissolution profiles of indinavir A and C. It was not possible to differentiate indinavir raw materials using this method. The drugs presented a maximum dissolution after 10 min (Fig. 2a). It only was possible to perform intrinsic dissolution using a

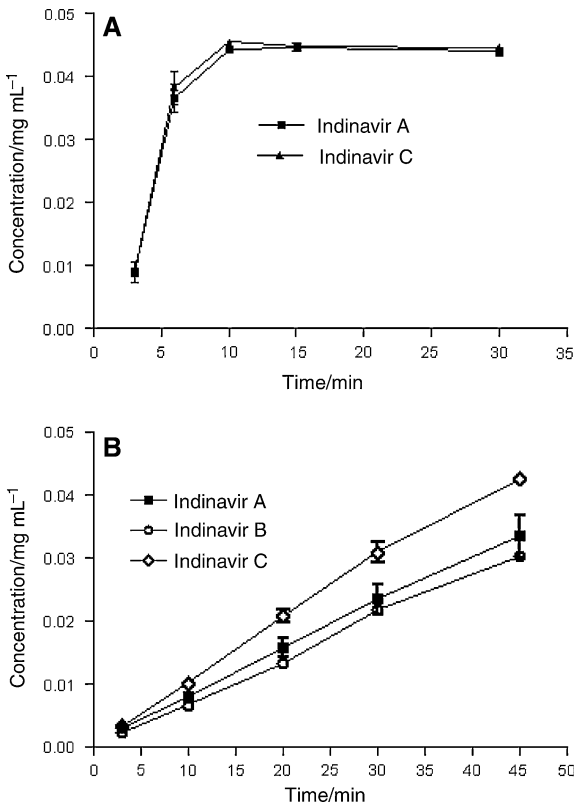

Fig. 2 Dissolution profile (**a**) and intrinsic dissolution (**b**) of indinavir A, B, and C. Graphics **a** and **b** show at each points of the standard deviation as vertical bar

compression force of 20 kN due to a failure in the compacting of indinavir under mechanical stress and consequently problems of disintegration in a dissolution medium during analysis, mainly for indinavir C. We observed a change in the pseudo-polymorphic forms for indinavir raw materials after a compression force of 20 kN. Sink condition was obtained in these experiments (Fig. 2b). The IDR expression (1) cited by Yu et al. [18] was applied to the linear regressions obtained in the raw materials (Indinavir A: $y = 0.0039x$ (± 0.0006); $r^2 = 0.995$, Indinavir B: $y = 0.0034x$ (± 0.0001); $r^2 = 0.996$, Indinavir C: $y = 0.0049x$ (± 0.0002); $r^2 = 0.996$).

$$\mathrm{IDR} = V * (\mathrm{d}C/\mathrm{d}t) * (1/A) \quad (1)$$

where IDR = intrinsic dissolution rate, V = volume of the dissolution medium, C = concentration of the drug, A = Area of the drug in disk, t = time.

Indinavir C (8.82 mg/min/cm^2) presented the highest IDR compared to indinavir A (7.02 mg/min/cm^2) and B (6.12 mg/min/cm^2). These data were coherent with studies of Yu et al. [18] and are in accordance with the criterion of high/low solubility classification cited by Kaplan [24], in which compounds presenting values below (0.10 mg/min/cm^2) exhibited a dissolution rate-limited absorption. The highest intrinsic dissolution rate for indinavir C can be justified due to the conversion of indinavir pseudo-polymorphs II into an amorphous state during the high compression prior to an intrinsic dissolution assay and observed in DSC curves. Indinavir A presented a high IDR in relation to indinavir B. Indinavir A also presented and a less grade of hydration than indinavir B observed in intrinsic dissolution assay and the Karl Fisher test. Pseudo-polymorphic forms with a lower grade of hydration can present a higher IDR as showed by some researches with hydrate forms. It was demonstrated a higher intrinsic rate for the anhydrous form of a substance and showed that it is more soluble in water than its corresponding monohydrate or dihydrate [7, 14, 25, 26].

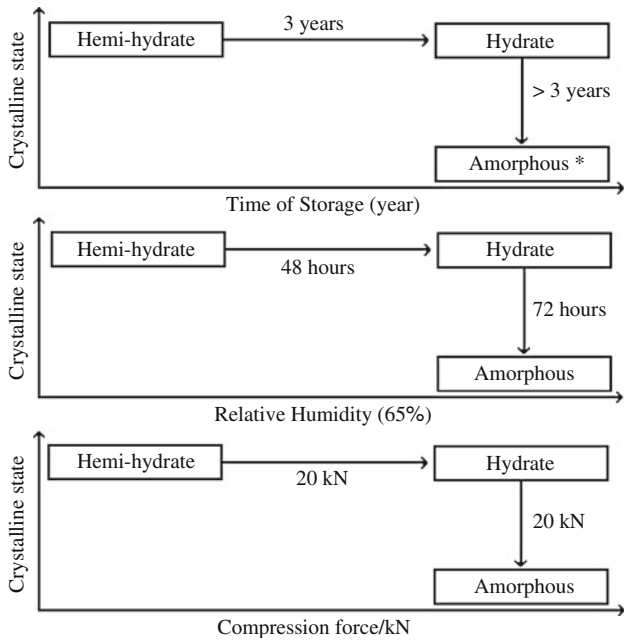

Fig. 3 Scheme of conversion in solid state for indinavir during some pharmaceutical processes. * Some indinavir raw materials presented amorphous state after 3 years of storage

Solid state stability of indinavir raw materials

DSC, Karl Fisher, and intrinsic dissolution data were important to establish a mnemonic scheme of conversion among the solid state forms of indinavir during some pharmaceuticals processes mainly, time of storage, exposure to high relative humidity, and compression force (Fig. 3).

Conclusions

We established the stability of indinavir sulfate during some pharmaceutical processes. The calorimetric data revealed the presence of two pseudo-polymorphic forms with different grades of hydration in the indinavir and its conversion into the amorphous state. In addition, a change was detected in raw materials due to relative humidity and storage conditions.

Special attention must be taken by the pharmaceutical industry during drastic process conditions such as high compression or compaction using mechanical equipment to promote the conversion of indinavir raw materials into pseudo-polymorphic form II or an amorphous state. These conditions can alter the physical–chemical properties, mainly dissolution rate, solubility in gastrointestinal fluids and consequently bioavailability of indinavir in patients.

The calorimetric and intrinsic dissolution were the main analytical techniques responsible in evaluating the quality of the indinavir raw materials and can be used in the qualification program of raw materials' suppliers, the validation of the manufacturing process and the stability of indinavir during a long period of storage.

Acknowledgements The authors thanks to the CNPq for its financial support with grant number 402665/05-08 of the funding of research n°54/2005—Pharmaceutical Assistance/MS/CNPq. The authors also want to thank the Laboratório Industrial Farmacêutico do Estado de Alagoas (LIFAL) in the persons of Maria Rocha C. Acioli, manager of the department of quality assurance, Denise M. M. França and Solange S. Moura pharmacists and Maria Cícera C. Santos for the technical support in the selection of the raw materials, NIR and Karl Fisher analysis and Hallison M. Pires and Flaviano Gomes of for the intrinsic dissolution assay at the IDEF/UFPB. Also thanks are given to the Instituto de Macromoléculas Prof. Eloisa Mano at the Universidade Federal do Rio de Janeiro for its XRPD analysis.

References

1. Brazilian Pharmacopeia. IV ed., supplement 1, p. 32. Brasil: DOU, seção 1, supplement n°209. Brasília: DF; 31 Oct 2005. p. 32.
2. Deeks SG, Smith M, Holodnly M, Kahn JO. HIV-1 protease inhibitors—a review for clinicians. J Am Med Assoc. 1997;277: 145–53.
3. Da Silva RMF, De Morais FPM, Nascimento TG, Macêdo RO, Neto PJR. Thermal characterization of indinavir sulfate using TG, DSC and DSC photovisual. J Therm Anal Calorim. 2009;95:965–8.
4. Murakami FS, Lang KL, Mendes C, Cruz AP, Filho MASC, Silva MAS. Physico-chemical solid-state characterization of omeprazole sodium: thermal, spectroscopic and crystallinity studies. J Pharm Biomed Anal. 2009;49:72–80.
5. Gandhi R, Pillai O, Thilagavathi R, Gopalakrishnan B, Kaul CL, Panchagnula R. Characterization of azithromycin hydrates. Eur J Pharm Sci. 2002;16:175–84.
6. Bartolomei M, Rodomonte A, Antoniella E, Minelli G, Bertocchi P. Hydrate modifications of the non-steroidal anti-inflammatory drug diclofenac sodium: solid-state characterisation of a trihydrate form. J Pharm Biomed Anal. 2007;45:443–9.
7. Grant DJW. Theory and origin of polymorphism. In: Brittain HG, editor. Polymorphism in pharmaceutical solids. New York: Marcel Dekker; 1999. p. 1–33.
8. Macêdo RO, Medeiros AFD, Santos AFO, Souza FS, Júnior IDB, Procópio JVV, et al. Thermal studies of pre-formulates of metronidazole obtained by spray drying technique. J Therm Anal Calorim. 2007;89:775–81.
9. Santos AFO, Macedo RO, Junior IDB, Souza FS, Pinto AFD, Santana DP. Application of thermal analysis in study of binary mixtures with metformin. J Therm Anal Calorim. 2008;93:361–4.
10. Medeiros ACD, Macedo RO, Cervantes NAB, Gomes APB. Technological quality determination of pharmaceutical disintegrant by DSC cooling and DSC photovisual. J Therm Anal Calorim. 2007;88:311–5.
11. Giron D. Thermal analysis and calorimetric methods in the characterisation of polymorphs and solvates. Thermochim Acta. 1995;248:1–49.
12. Halebian J. Characterization of habits and crystalline modification of solids and their pharmaceutical applications. J Pharm Sci. 1975;64:1269–88.
13. Brittain HG. Methods for characterization of polymorphs and solvates. In: Brittain HG, editor. Polymorphism in pharmaceutical solids, vol. 95. New York: Marcel Dekker; 1999. p. 227–79.
14. Vrecer F, Vrbinc M, Meden A. Characterization of piroxicam crystal modifications. Int J Pharm. 2003;256:3–15.
15. Vogt FG, Brum J, Katrincic LM, Flach A, Socha JM, Goodman RM, et al. Physical, crystallographic, and spectroscopic characterization of a crystalline pharmaceutical hydrate: understanding the role of water. Cryst Growth Des. 2006;6:2333–54.
16. Chan HK, Grant DJ. Influence of compaction on disk intrinsic dissolution rates. Int J Pharm. 1989;57:117–24.
17. Jinno J, Crison JR, Amidon GL. Dissolution of ionizable water-insoluble drugs: the combined effect of pH and surfactant. J Pharm Sci. 2000;89:268–74.
18. Yu LX, Carlin AS, Amidon GL, Hussain AS. Feasibility studies of utilizing intrinsic dissolution rate to classify drugs. Int J Pharm. 2004;270:221–7.
19. The Merck Index. An encyclopedia of chemicals, drugs, and biologicals, 12th ed. Whitehouse Station, NJ: Merk & Co.; 1996.
20. Demir AS, Hamamci H, Doganel F, Ozgul E. Chemoenzymatic synthesis of (1*S*, 2*R*)-1-amino-2-indanol, a key intermediate of HIV protease inhibitor, indinavir. J Mol Catal B: Enzym. 2000;9: 157–61.
21. Singh P, Premkumar L, Mehrotra R. Evaluation of thermal stability of indinavir sulphate using diffuse reflectance infrared spectroscopy. J Pharm Biomed Anal. 2008;47:248–54.
22. Kaul N, Agrawal H, Paradkar AR, Mahadik KR. The ICH guidance in practice: stress degradation studies on indinavir sulphate and development of a validated specific stability-indicating HPTLC assay method. IL FARMACO. 2004;59:729–38.
23. Czarnik-Matusewicz B, Pilorz S. Study of the temperature-dependent near-infrared spectra of water by two-dimensional correlation spectroscopy and principal components analysis. Vib Spectrosc. 2006;40:235–45.
24. Kaplan SA. Biopharmaceutical considerations in drug formation design and evaluation. Drug Metab Rev. 1972;1:15–34.
25. Kobayashi Y, Ito S, Itai S, Yanamoto K. Physicochemical properties and bioavailability of carbamazepine polymorphs and hydrate. Int J Pharm. 2000;193:137–46.
26. Di Martino P, Barthélémy C, Palmieri GF, Martelli S. Physical characterization of naproxen sodium hydrate and anhydrate forms. Eur J Pharm Sci. 2001;14:293–300.